

Carbon quantum dots of *Moringa oleifera* with bactericidal action

Pontos quânticos de carbono de óleo de *Moringa oleifera* com ação bactericida

Alexandre Rodrigues Simões

ORCID: <https://orcid.org/0009-0008-8912-5614>
Centro Universitário de Adamantina (FAI), Brasil
E-mail: simoes@fai.com.br

Alexandre Teixeira de Souza

ORCID: <https://orcid.org/0000-0003-0357-0925>
Centro Universitário de Adamantina (FAI), Brasil
E-mail: alteiso@fai.com.br

Eduardo César Meurer

ORCID: <https://orcid.org/0000-0003-4835-7773>
Universidade Federal do Paraná (UFPR), Brasil
E-mail: eduardo.meurer@ufpr.br

Évelin Lemos de Oliveira

ORCID: <https://orcid.org/0000-0002-8208-0950>
Universidade Federal do Paraná (UFPR), Brasil
E-mail: elemosoliveira01@gmail.com

Mara Heloisa Neves Olsen Scaliante

ORCID: <https://orcid.org/0000-0001-9090-9274>
Universidade Estadual de Maringá (UEM), Brasil
E-mail: msnoscaliante2@uem.br

Rodrigo Renolfi Erler

ORCID: <https://orcid.org/0009-0009-4202-8187>
Centro Universitário de Adamantina (FAI), Brasil
E-mail: rodrigoerler@fai.com.br

Wilker Caetano

ORCID: <https://orcid.org/0000-0002-9402-8324>
Universidade Estadual de Maringá (UEM), Brasil
E-mail: wcaetano@uem.br

RESUMO

Neste trabalho foram sintetizados pontos quânticos de carbono (PQC) utilizando um reator hidrotérmico. O precursor dos PQC foi o óleo da semente de *Moringa oleifera*, extraído com etanol 1:8 (m/v), via extração assistida por ultrassom (50 °C, 30 min) e purificado através de um rotaevaporador (50 °C, 50 rpm) para remoção do solvente e então centrifugado (12000 rpm, 10 min). O óleo foi transferido para uma cápsula de Teflon colocada em um reator inox e aquecida na mufla (210 °C, 24 h). Os PQC sintetizados foram centrifugados (12000 rpm, 10 min) e filtrados em membrana de 0.22 µm, apresentando uma alta fluorescência em luz ultravioleta (365 nm) e ativados fotodinamicamente com luz visível branca, promovendo uma inibição para a bactéria Gram-positiva *Staphylococcus aureus*, uma das causadoras das infecções de pele. Nas últimas décadas o uso inadequado de antibióticos promoveu um aumento da resistência de bactérias, aumentando a mortalidade em humanos e animais, assim o desenvolvimento de um nanomaterial com propriedades antimicrobianas é essencial para a saúde e o bem estar da população. Esse processo foi realizado através de uma rota simples, barata e sustentável.

Palavras-chave: Nanotecnologia; Oxigênio singlete; Drogas; Saúde.

ABSTRACT

In this work, carbon quantum dots (CQDs) were synthesized using a hydrothermal reactor. The precursor for the CQDs was *Moringa oleifera* seed oil, extracted using a 1:8 ethanol-to-mass ratio through ultrasound-assisted extraction (50 °C, 30 min). The extract was then purified using a rotary evaporator (50 °C, 50 rpm) to remove the solvent, followed by centrifugation (12,000 rpm, 10 min). Subsequently, the oil was transferred to a Teflon-lined capsule within a stainless-steel reactor and heated in a muffle furnace (210 °C, 24 h). The synthesized CQDs were then centrifuged (12,000 rpm, 10 min) and filtered through a 0.22 µm membrane. These CQDs exhibited high fluorescence and, when activated photodynamically with white visible light, showed the ability to inhibit the growth of the Gram-positive bacterium *Staphylococcus aureus*, a common cause of skin infections. In recent decades, the inappropriate use of antibiotics has led to increased bacterial resistance, resulting in higher mortality rates in humans and animals. Therefore, the development of nanomaterials with antimicrobial properties, through a simple, cost-effective, and sustainable route, is essential for public health and safety.

Keywords: Nanotechnology; Singlet oxygen; Drugs; Health.

INTRODUCTION

Staphylococcus aureus (*S. aureus*) is a bacterial pathogen found on the skin, nasal passages, and mucous membranes of healthy individuals, which globally can promote human infection, especially in individuals with low immune resistance. These bacteria naturally exhibit the characteristic of producing biofilms composed of proteinaceous polysaccharides, impeding the action of leukocytes in the body's defense and the efficacy of antimicrobial agents (GRUNDMANN *et al.*, 2006; WERTHEIM *et al.*, 2005). LINZ and colleagues (2023) reported that, in 2019, 30.9% of the 7.7 million infectious deaths worldwide were associated with the bacterium *S. aureus*, along with *Escherichia coli*, *Streptococcus pneumoniae*, *Klebsiella pneumoniae*, and *Pseudomonas aeruginosa*. Considering only the bacterium *S. aureus*, it represents the leading cause of death in 135 countries, resulting in 1,105,000 deaths in 2019.

The antimicrobial resistance of various drug types associated with the abuse and misuse of antibiotics by patients and livestock, or even released into the environment irresponsibly, has become a global health problem (ROCA *et al.*, 2015). The development of new perspectives involving the prevention and treatment of infectious diseases is essential. Among them, the use of self-disinfecting materials such as antimicrobial photodynamic inactivation (aPDI) stands out. This method employs a non-toxic photosensitizer with a wavelength typically in visible light, resulting in the generation of singlet oxygen ($^1\text{O}_2$) and other reactive oxygen species (ROS) (ST. DENIS *et al.*, 2011).

Nanotechnology has led to the development of materials with therapeutic applications, including bioimaging, photodynamic therapy, photocatalysis, and nanomedicine, such as quantum dots, doped nanoparticles, and polymer dots (GUPTA *et al.*, 2019; NIE *et al.*, 2020). Carbon quantum dots (CQDs) are zero-dimensional carbon-based nanoparticles with a size smaller than 10 nm. They have rapidly evolved in recent decades, exhibiting distinctive characteristics, such as excellent photodynamic sensitizing potential for use in photodynamic inactivation, biocompatibility, adjustable photoluminescence, excellent optical and electronic properties, chemical stability, water solubility, easy surface functionalization, ease of production, low cost, high storage stability, and low toxicity (GAO *et al.*, 2022; XIE *et al.*, 2019). The Royal Swedish Academy of Sciences awarded the 2023 Nobel Prize in Chemistry for the discovery and synthesis of quantum dots to YU & SCHANZE (2023).

There are two commonly used approaches for preparing CQDs (ZHENG *et al.*, 2015). The top-down technique involves the use of large-scale carbon materials, such as carbon nanotubes and graphite ashes, which are decomposed into small CQDs, ranging from macro to nano-scale. Among the top-down techniques, laser ablation, arc discharge, plasma treatment, electrochemical oxidation, and others are notable (JUNG *et al.*, 2022; MENG *et al.*, 2019). The bottom-up approach is carried out through the pyrolysis or carbonization of small organic molecules or by stepwise chemical fusion of small aromatic molecules. Chemical processes such as hydrothermal, pyrolysis, combustion, ultrasonic, microwave irradiation, thermal, and biogenic procedures are techniques within the bottom-up approach (SHEN *et al.*, 2022; WANG *et al.*, 2023; ZHUANG *et al.*, 2021).

Different precursors have been employed in the production of CQDs; however, in recent years, the pursuit of renewable, more affordable, and eco-friendly sources has been the subject of various studies due to their sustainable development (GOSWAMI *et al.*, 2022; HOAN *et al.*, 2019). ARKAN and colleagues (2018) prepared carbon quantum dots from walnut oil with a high quantum yield through a hydrothermal synthesis.

Moringa oleifera (MO) is a medium-sized, fast-growing tree native to northern India, introduced in tropical countries for its drought resistance and year-round productivity. It is one of the 13 species in the *Moringaceae* genus. Due to its versatility and properties, numerous studies have been conducted using its seeds, leaves, roots, and flowers with applications in the food, pharmaceutical, cosmetic, and nutritional fields. These compounds are rich in antioxidants and, therefore, possess protective and

therapeutic properties (FAKAYODE & AJAV, 2016; GHARSALLAH *et al.*, 2021; UEDA YAMAGUCHI *et al.*, 2021; VENTURA *et al.*, 2021; ZHONG *et al.*, 2018). MO seeds contain oil (35-45%) with a high concentration of oleic acid (>73%) (AYERZA(H), 2019).

In this study, the raw material used was the oil from *M. oleifera* seeds, and typically, during the process of CQD synthesis, some properties of the precursor material are retained, which favors the development of this new nanomaterial (WU *et al.*, 2021). The literature presents few works involving the production of CQDs using vegetable oil as a raw material.

The main objective of this study was to synthesize CQDs from *Moringa oleifera* seed oil using the hydrothermal method, in a sustainable manner, with antimicrobial photodynamic activity activated by visible light, targeting the bacterium *Staphylococcus aureus*.

MATERIALS and METHODS

Samples and reagents

The seeds of *Moringa oleifera* (MO) were obtained from a supplier located in the city of Fortaleza, Ceará (latitude 3° 43' 6" S and longitude 38° 32' 36" W). Initially, the seeds underwent a manual peeling process, followed by grinding and sieving through a stainless-steel mesh with a 30-mesh size and 0.595 mm opening for powder extraction and classification. Ten grams of the powder were weighed and placed in an oven at 105 °C until moisture removal. The powder was then transferred to polypropylene bags for storage and subsequent use. Absolute ethanol (99.5%) from Dinâmica, Brazil, was used. Mueller-Hinton agar (MH) and tryptic soy broth (TSB) were acquired from KASVI (São José dos Pinhais, Brazil). The bacterial standard culture used was *Staphylococcus aureus* ATCC 25923.

Ultrasound-Assisted Extraction (UAE)

The ultrasound-assisted extraction (UAE) process of *Moringa oleifera* oil was carried out and adapted according to the methodology of ZHONG and colleagues (2018). Ethanol was chosen for this process as it is an environmentally friendly and cost-effective solvent, generating minimal waste. An ultrasonic bath (100W, 40 kHz, Skymen, China) was employed for the oil extraction. Ten grams of powder were transferred to an

Erlenmeyer flask, and the solvent (ethanol) was added at a mass/volume ratio of 1:8, then placed in a water bath for 30 minutes. The bath temperature ($50\text{ }^{\circ}\text{C} \pm 1\text{ }^{\circ}\text{C}$) was controlled using a water circulation system and a digital thermometer. The extract was allowed to settle for 12 hours and then filtered using Whatman filter paper to separate large particles. Subsequently, the ethanol removal process was conducted using a micro processed rotary evaporator (Quimis, W344M2, Brazil) at $50\text{ }^{\circ}\text{C}$ (50 rpm) equipped with a vacuum pump, with the recovered ethanol being reused. The final solution containing the oil was placed in an oven at $45\text{ }^{\circ}\text{C}$ for 24 hours to remove the remaining solvent.

Synthesis of Carbon Quantum Dots (CQDs)

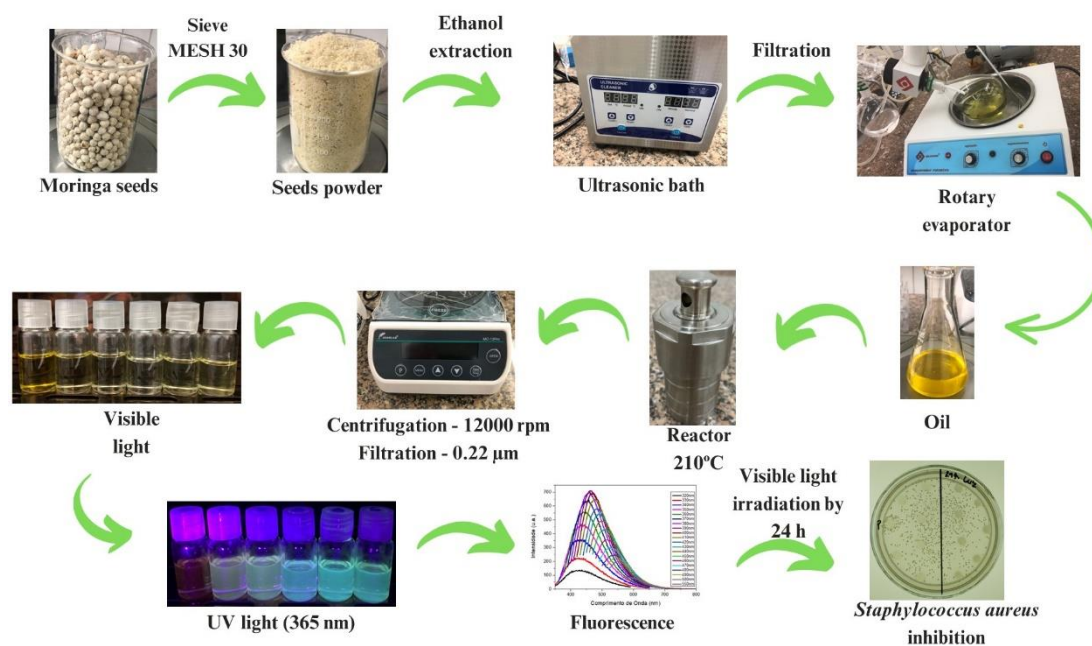
The synthesis methodology employed in this study involved the bottom-up approach through the hydrothermal method to synthesize CQDs using *M. oleifera* oil. For each experiment, 3 g of oil were centrifuged in a centrifuge (Joanlab, MS-12Pro, China) at 12000 rpm for 10 minutes and then transferred to a 25 mL Teflon-coated stainless-steel reactor, heated in an oven at $210\text{ }^{\circ}\text{C}$, and cooled to room temperature. Five experiments were conducted with synthesis times of 2 hours, 4 hours, 8 hours, 12 hours, and 24 hours. The produced CQDs were centrifuged at 12000 rpm for 10 minutes and purified through a $0.22\text{ }\mu\text{m}$ membrane. They were then examined under an ultraviolet (UV) lamp with a wavelength of 365 nm, where fluorescence was observed, indicating the synthesis of CQDs. In this method, the synthesis was simple and direct, without involving sophisticated equipment. All experiments were conducted in triplicate.

Bacterial Inactivation of *S. aureus*

The *Staphylococcus aureus* ATCC 29213 microorganism was cultivated in TSB broth at $37\text{ }^{\circ}\text{C}$ for 24 hours. Tests were performed using a standardized cell density in tubes with 0.9% sterile saline solution, with turbidity identical to that of the McFarland 0.5 tube ($1 \times 10^8\text{ CFU mL}^{-1}$) from a serial dilution. Petri dishes with Mueller-Hinton Agar (MH) were prepared following the preparation and sterilization protocol. After solidification, $100\text{ }\mu\text{L}$ microbial suspensions were added to the plates, followed by surface spreading technique with a DRIGALSKI loop. After the suspension was absorbed by the agar, $10\text{ }\mu\text{L}$ of *M. oleifera* oil and CQDs were added at various points on the plate's surface. The plates were then incubated in a growth chamber at $37\text{ }^{\circ}\text{C}$, with a homemade white LED light source (OSRAM brand, 20W) placed 30 cm above the plates. Each plate

received light irradiation for a predetermined time (2 hours, 12 hours, and 24 hours) and then incubated for 24 hours at 37 °C. Experimental groups with light irradiation were compared with their respective control groups that did not receive any light irradiation. All assays were performed in quadruplicate. Figure 1 illustrates the flowchart of the carbon quantum dots (CQDs) synthesis, starting with *Moringa oleifera* seeds.

Figure 1 - Synthesis of carbon quantum dots (CQDs) derived from *M. oleifera* oil.



Sources: authors (2023).

UV-Visible Electronic Absorption

UV-Visible electronic absorption spectra were obtained by adding 2 mL of the sample to a quartz cuvette with a 1 cm optical path length, and measurements were conducted on the Cary 60 spectrophotometer (Agilent, USA) with a wavelength scan range from 200 to 800 nm.

Fluorescence Emission

Fluorescence emission spectra were acquired by adding 2 mL of the sample to a quartz cuvette with a 1 cm optical path length, and measurements were performed using the Cary Eclipse fluorescence spectrophotometer (Agilent, USA) with an excitation wavelength range from 320 to 550 nm, a slit width of 5-5, and a scan wavelength (excitation wavelength + 20 nm) up to 800 nm.

Instrumentation

The UV-Visible absorption spectra of the CQDs were recorded using the Cary 60 UV-Visible spectrophotometer (Agilent, USA) with a quartz cuvette having a 1 cm optical path length. The fluorescence spectrum was obtained using the Cary Eclipse spectrophotometer (Agilent, USA). The functional groups of the CQDs were analyzed by Fourier Transform Infrared Spectroscopy (FTIR) using a Shimadzu IRAffinity 1 instrument.

RESULTS AND DISCUSSION

M. oleifera oil was thermally treated at 210 °C for various durations (2 h, 4 h, 8 h, 12 h, and 24 h) using the hydrothermal method. Characterization was performed on the pure oil sample and the CQD sample (24 h), as it exhibited the highest fluorescence intensity and was used for the antimicrobial photodynamic inactivation (aPDI) assay.

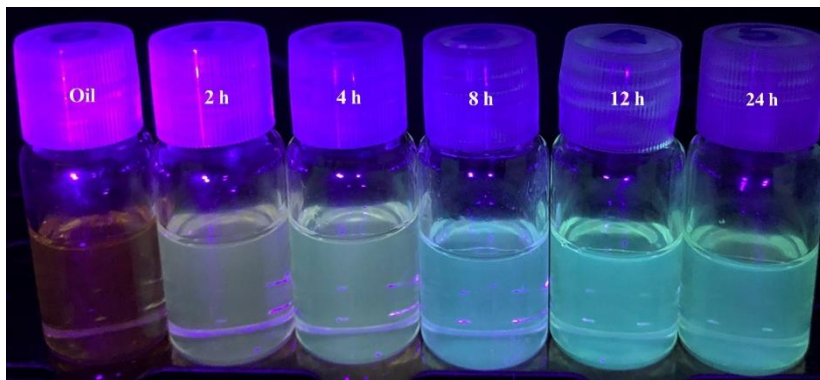
Figure 2 displays the samples under visible light irradiation, and Figure 3 shows the samples under UV light irradiation (365 nm), illustrating the fluorescence emissions of the carbon quantum dots.

Figure 2 - Sample of pure oil and CQD at different heat treatment times at 210°C under visible light irradiation (white light).



Source: authors (2023).

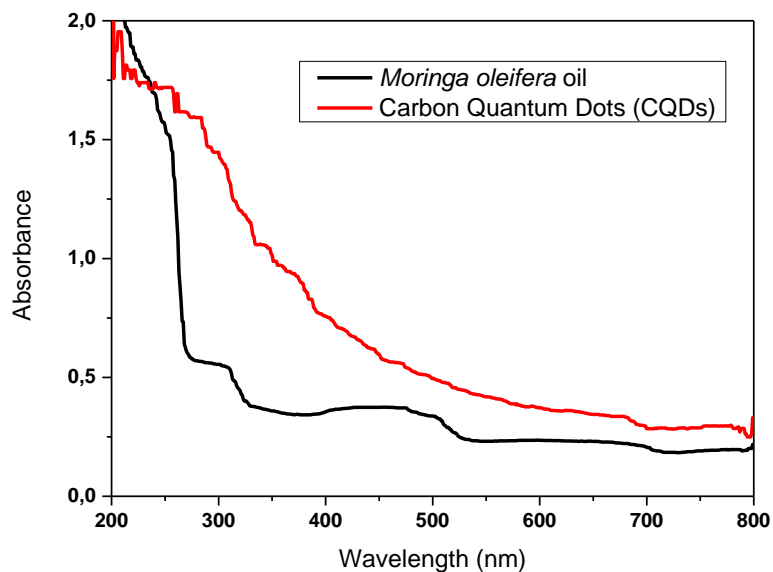
Figure 3 - Samples of pure oil and CQDs at different heat treatment times at 210 °C under UV irradiation (365 nm).



Source: authors (2023).

M. oleifera oil exhibited a strong absorption band in the ultraviolet region, characteristic of C=O transitions, and a band in the 400 to 500 nm range related to carotenoid absorption, responsible for the oil's yellowish coloration (Figure 4). The CQDs have an absorption band that starts in the 500 nm region extending into the ultraviolet region. The optical absorption spectrum of quantum dots typically consists of two main bands, peaking around 250 and 350 nm. This spectrum is consistently reported for doped quantum dots, regardless of the synthesis procedure. However, in the case of simple samples where no heteroatoms are added as precursors or those atoms do not participate in the formation of specific optical centers, the near-UV band is not known (CARBONARO *et al.*, 2018).

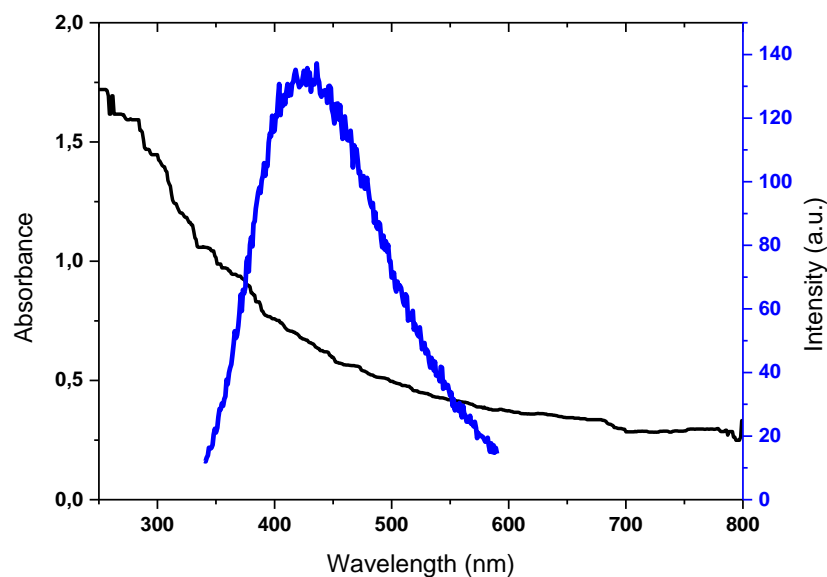
Figure 4 - UV-vis electronic absorption spectra of *Moringa oleifera* oil and CQD.



Source: authors (2023).

Figure 5 depicts the relationship between absorbance and light intensity as a function of the wavelength of the CQDs produced from *M. oleifera* oil. There is a peak in the fluorescence emission intensity at 436 nm.

Figure 5 - UV-vis electronic absorption and fluorescence emission spectra of CQDs.

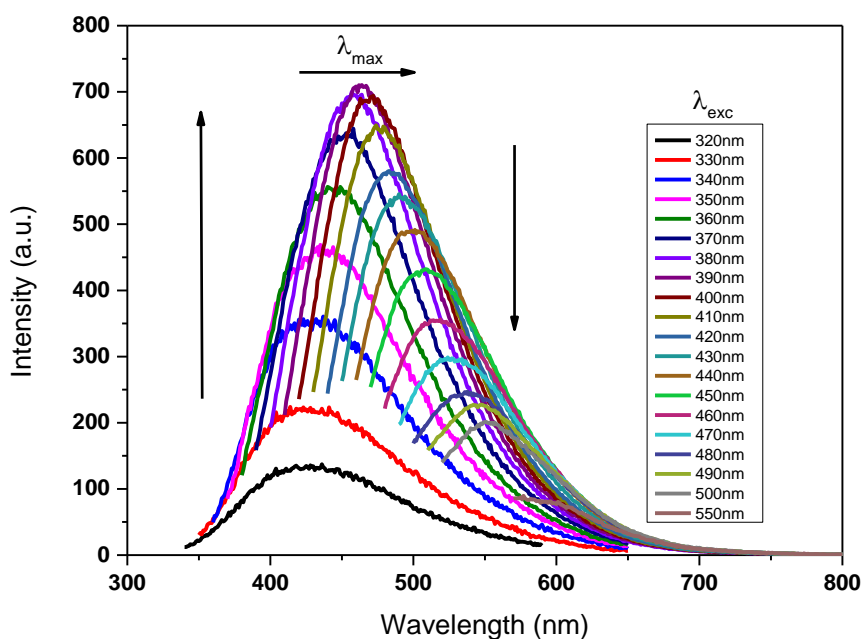


Source: authors (2023).

The intensity of photoluminescence is directly associated with the excited absorption band, showing higher emission intensity when the π - π^* band is stimulated. On the other hand, lower intensity occurs when the excitation takes place within the far ultraviolet range, particularly within the π - π^* absorption band. In this context, the appearance of photoluminescence peaks depends on the structural composition of carbon dots and the presence of various elements on their surface (CARBONARO *et al.*, 2019).

Figure 6 presents the fluorescence emission spectrum of the CQDs. Between excitation wavelengths of 320 to 400 nm, there is an increase in fluorescence emission, and from 400 to 550 nm, there is a decrease in fluorescence emission. The excitation-dependent emission property of the synthesized CQDs is attributed to the existence of different particle sizes, various defects and surface states, and the origin of CQDs' fluorescence still requires further discussion (ATCHUDAN *et al.*, 2021; KALANIDHI & NAGARAAJ, 2021).

Figure 6 - CQD fluorescence emission spectrum, excitation wavelength ranging from 320 to 550 nm.

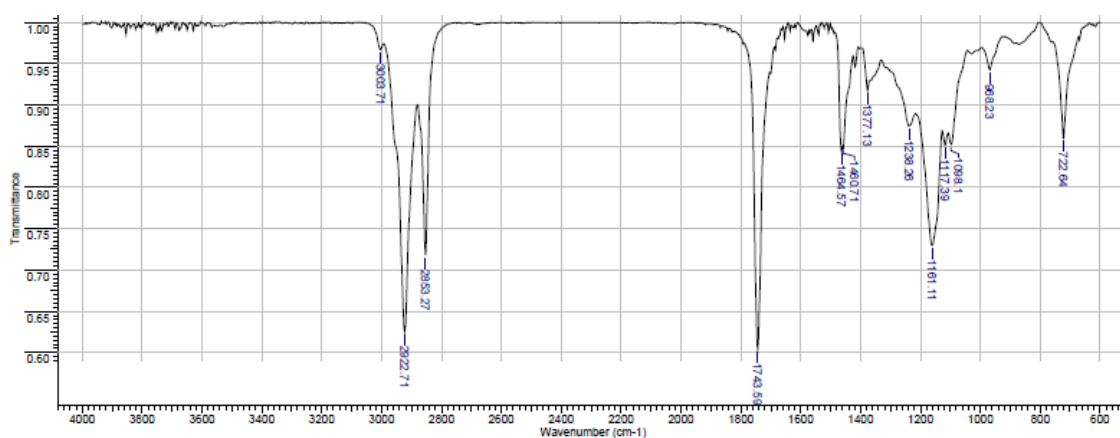


Source: authors (2023).

FTIR spectroscopy was used to identify the functional groups in *M. oleifera* seeds, before and after hydrothermal treatment, and no significant changes in their chemical structure were observed after thermal treatment. The spectrum in Figure 7 illustrates a

variety of functions of the groups forming the molecular complex of the CQDs.

Figure 7 - FTIR spectra of the PQCs synthesized from *Moringa oleifera* oil.



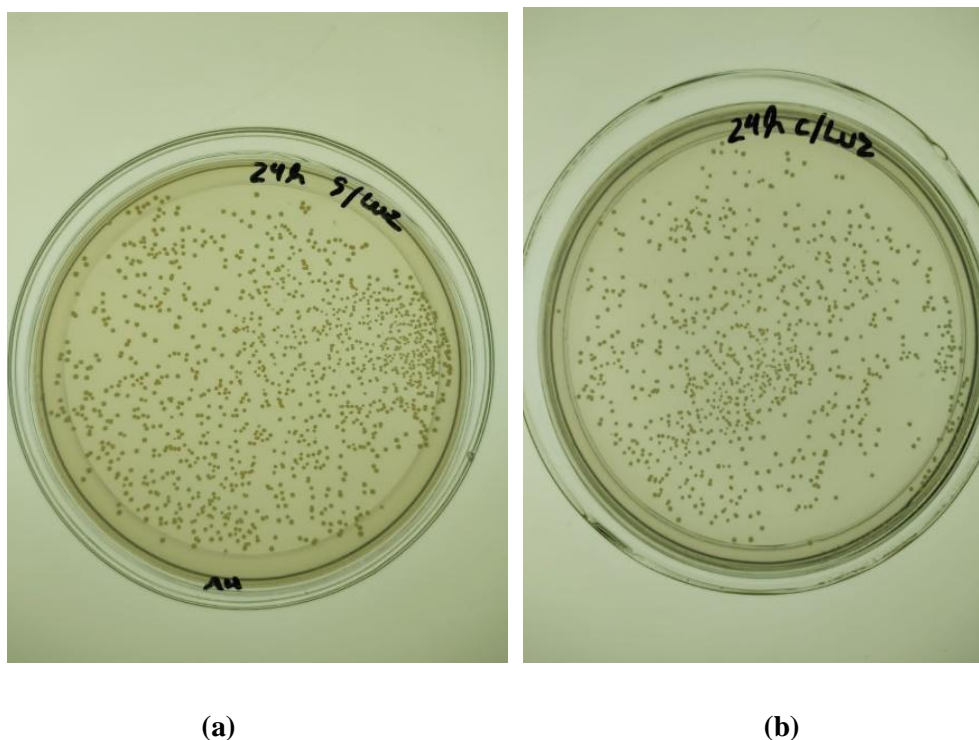
Source: authors (2023).

The absorption band at 2922 cm^{-1} can be attributed to the fatty acids present in the oil as it corresponds to the symmetric and asymmetric stretching of $\text{CH}(\text{CH}_2)$ groups, commonly found in these types of compounds (BAPTISTA *et al.*, 2017). The peak at 1743 cm^{-1} corresponds to the stretching of $\text{C}=\text{O}$ bonds in the ester functional groups of lipids and fatty acids (Timilsena *et al.*, 2019), and a band at 1460 cm^{-1} is related to the $\text{C}=\text{C}$ aromatic bond. The band at 1161 cm^{-1} is assigned to the esters of diacylglycerol and represents asymmetric stretches of $\text{C}-\text{C}(=\text{O})$, $-\text{O}$, and $\text{O}-\text{C}-\text{O}$ bonds (WILTSHIRE *et al.*, 2022). The band at 722 cm^{-1} is due to the asymmetric deformation of the CH_2 group (MOREIRA *et al.*, 2020).

To study the inhibition of Gram-positive bacterial growth using the CQDs, various experiments were conducted to optimize antibacterial photodynamic inactivation. Initially, colony-forming units (CFUs) of *S. aureus* were observed in an environment with visible light and in the absence of light, without the presence of *M. oleifera* oil and CQDs.

In Figures 8a and 8b, the growth of CFUs is observed in the absence and presence of light irradiation, respectively, incubated at $37\text{ }^\circ\text{C}$ for a period of 24 hours.

Figure 8 - a) *S. aureus* in an environment without light irradiation; **b)** *S. aureus* with visible light irradiation (24h).

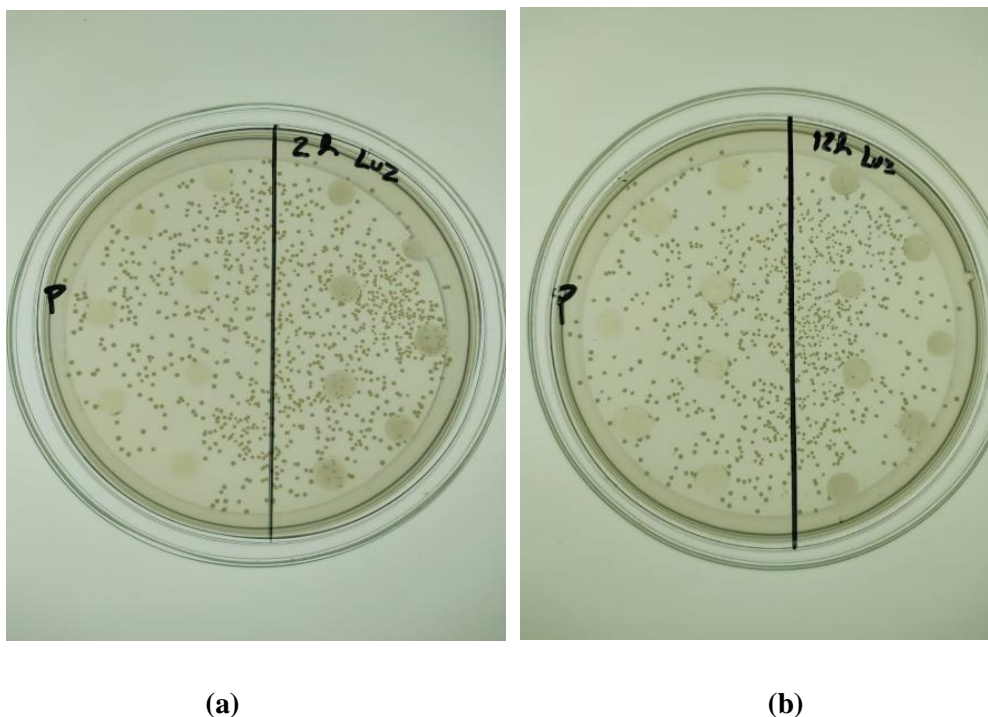


Source: authors (2023).

The synthesized CQDs were added to Petri dishes containing *S. aureus* bacteria. The Petri dish was divided into two regions, with *M. oleifera* oil dripped on the left side and CQDs on the right side, each drop containing a volume of 10 μL . When exposed to 2 hours of visible light irradiation (Figure 9a), CFUs developed in the areas of the CQDs, while in the oil area, there was a slight inhibition. This is due to the antioxidant properties present in *M. oleifera* oil (GUEDES *et al.*, 2022).

In Figure 9b (12 hours of visible light), there is inhibition of *S. aureus* in both the oil and CQD areas, with the effect being more predominant in the presence of visible light irradiation. The CQDs release high levels of $^1\text{O}_2$ when exposed to white LED light, which can kill up to 97% of *S. aureus* (WU *et al.*, 2022).

Figure 9 - a) *S. aureus* with 2 h of visible light irradiation and **b)** *S. aureus* with 12 h of visible light irradiation.



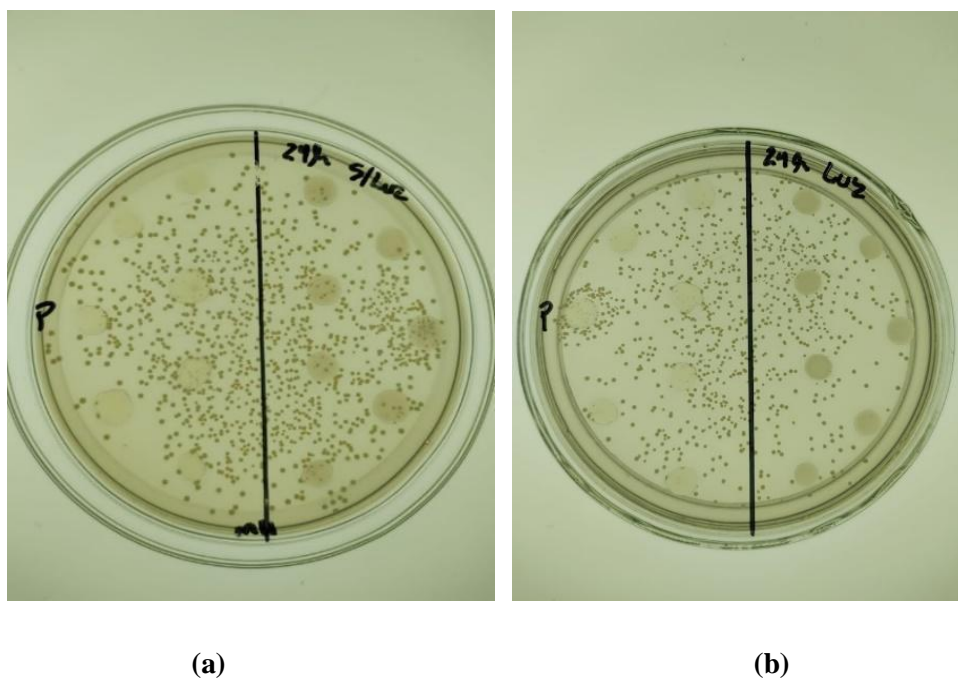
Source: authors (2023).

Figure 10a, without exposure to visible light, shows growth of CFUs in both oil (lower intensity) and CQD areas (higher intensity). When exposed to 24 hours of visible light, there is a significant inhibition of CFUs in the CQD areas, confirming their photodynamic bacterial inactivation effect, while in the region where *M. oleifera* oil was applied, there was a slight inhibition.

Photodynamic antimicrobial activity (PAA) is based on the triggered generation, by visible light irradiation, of reactive oxygen species (ROS) and redox species, responsible for antimicrobial action against various pathogens.

ROS, such as singlet oxygen, superoxide anion, and hydroxyl radicals, have a broad spectrum of activity and can simultaneously attack various biomolecular sites in microbial targets (e.g., proteins, lipids, and nucleic acids). This nonspecific damage makes it difficult for pathogens to develop resistance; therefore, PAA represents a promising strategy for destroying antibiotic-resistant microorganisms (RUIZ *et al.*, 2022; WAINWRIGHT *et al.*, 2017).

Figura 10 - a) *S. aureus* without visible light irradiation and **b)** *S. aureus* with 24 h of visible light irradiation.



Source: authors (2023).

Table 1 presents the CFU count conducted in the experiments, where exposure times to visible light (2 h, 12 h, and 24 h) were varied using both oil and CQDs, as well as the Control (without visible light).

Table 1: Colony-Forming Units (CFUs) of *S. aureus* present in the oil and CQD areas at 37°C, under different durations of light irradiation.

Light irradiation time	2 h	12 h	24h
UFC mL ⁻¹			
Oil	0.85x10 ⁵ ± 0.16*	3.40x10 ⁵ ± 0.30*	4.40x10 ⁵ ± 0.34*
CQD (With light)	-	-	5.40x10 ⁵ ± 0.61*
Oil (Without light)	-	-	4.30x10 ⁵ ± 0.73*
CQD	8.10x10⁵ ± 0.72*	2.10x10⁵ ± 0.53*	0*

*Averages performed in quadruplicate. Source: authors (2023).

With the increase in light exposure time (2 h to 24 h), CFUs showed growth in the oil areas. However, when observing the CQD areas, there was a decrease in CFUs with

the extended duration of visible light irradiation. After 12 h of visible light irradiation, CFUs were reduced by 74%, and after 24 h, there was 100% inhibition.

CONCLUSION

This study demonstrated the antibacterial effects of CQDs synthesized in a hydrothermal reactor using *Moringa oleifera* oil as a precursor, through a low-cost, easy-to-operate, sustainable, and environmentally friendly process. CQDs exhibited high fluorescence and inhibition against the Gram-positive bacterium *Staphylococcus aureus* when activated by white light for a 24-hour irradiation period. CQDs show great potential for use in open environments where natural visible light predominates.

Acknowledgments

This work was supported by the Coordenação de Aperfeiçoamento de Pessoal de Nível Superior (CAPES), the Fenn Mass Spectrometry Laboratory at UFPR Jandaia do Sul, the Universidade Estadual de Maringá (UEM), and the Centro Universitário de Adamantina (FAI).

REFERENCES

- ARKAN, E., BARATI, A., RAHMANPANA, M., HOSSEINZADEH, L., MORADI, S., & HAJIALYANI, M. (2018). Green synthesis of carbon dots derived from walnut oil and an investigation of their cytotoxic and apoptogenic activities toward cancer cells. *Advanced Pharmaceutical Bulletin*, 8(1), 149–155. <https://doi.org/10.15171/apb.2018.018>
- ATCHUDAN, R., JEBAKUMAR IMMANUEL EDISON, T. N., SHANMUGAM, M., PERUMAL, S., SOMANATHAN, T., & LEE, Y. R. (2021). Sustainable synthesis of carbon quantum dots from banana peel waste using hydrothermal process for in vivo bioimaging. *Physica E: Low-Dimensional Systems and Nanostructures*, 126. <https://doi.org/10.1016/j.physe.2020.114417>
- AYERZA(H), R. (2019). Seed characteristics, oil content and fatty acid composition of moringa (*Moringa oleifera* Lam.) seeds from three arid land locations in Ecuador. *Industrial Crops and Products*, 140. <https://doi.org/10.1016/j.indcrop.2019.111575>

CARBONARO, C. M., CHIRIU, D., STAGI, L., CASULA, M. F., THAKKAR, S. V., MALFATTI, L., SUZUKI, K., RICCI, P. C., & CORPINO, R. (2018). Carbon Dots in Water and Mesoporous Matrix: Chasing the Origin of their Photoluminescence. *Journal of Physical Chemistry C*, 122(44), 25638–25650. <https://doi.org/10.1021/acs.jpcc.8b08012>

CARBONARO, CORPINO, SALIS, MOCCI, THAKKAR, OLLA, & RICCI. (2019). On the Emission Properties of Carbon Dots: Reviewing Data and Discussing Models. *C — Journal of Carbon Research*, 5(4), 60. <https://doi.org/10.3390/c5040060>

FAKAYODE, O. A., & AJAV, E. A. (2016). Process optimization of mechanical oil expression from Moringa (*Moringa oleifera*) seeds. *Industrial Crops and Products*, 90, 142–151. <https://doi.org/10.1016/j.indcrop.2016.06.017>

GAO, X., ZHANG, Y., FU, Z., & CUI, F. (2022). Preparation of lysosomal targeted fluorescent carbon dots and its applications in multi-color cell imaging and information encryption. *Optical Materials*, 131. <https://doi.org/10.1016/j.optmat.2022.112701>

GHARSALLAH, K., REZIG, L., MSAADA, K., CHALH, A., & SOLTANI, T. (2021). Chemical composition and profile characterization of moringa oleifera seed oil. *South African Journal of Botany*, 137, 475–482. <https://doi.org/10.1016/j.sajb.2020.11.014>

GOSWAMI, J., ROHMAN, S. S., GUHA, A. K., BASYACH, P., SONOWAL, K., BORAH, S. P., SAIKIA, L., & HAZARIKA, P. (2022). Phosphoric acid assisted synthesis of fluorescent carbon dots from waste biomass for detection of Cr(VI) in aqueous media. *Materials Chemistry and Physics*, 286. <https://doi.org/10.1016/j.matchemphys.2022.126133>

GRUNDMANN, H., AIRES-DE-SOUSA, M., BOYCE, J., & TIEMERSMA, E. (2006). Emergence and resurgence of meticillin-resistant *Staphylococcus aureus* as a public-health threat. *www.TheLancet.Com*, 368. <https://doi.org/10.1016/S0140>

GUEDES, C. C. DA S., BUONAFINA-PAZ, M. D. S., ROCHA, S. K. L., COELHO, L. C. B. B., NAVARRO, D. M. DO A. F., NEVES, R. P., NAPOLEÃO, T. H., DE OLIVEIRA, A. P. S., DA SILVA, P. M., & PAIVA, P. M. G. (2022). Antimycotic potential of protein preparation and fixed oil obtained from *Moringa oleifera* seeds against *Trichophyton tonsurans*. *South African Journal of Botany*, 150, 443–450. <https://doi.org/10.1016/j.sajb.2022.08.023>

GUPTA, N., RAI, D. B., JANGID, A. K., & KULHARI, H. (2019). Use of nanotechnology in antimicrobial therapy. In *Methods in Microbiology* (Vol. 46, pp. 143–172). Academic Press Inc. <https://doi.org/10.1016/bs.mim.2019.04.004>

HOAN, B. T., TAM, P. D., & PHAM, V. H. (2019). Green Synthesis of Highly Luminescent Carbon Quantum Dots from Lemon Juice. *Journal of Nanotechnology*, 2019. <https://doi.org/10.1155/2019/2852816>

JUNG, H., SAPNER, V. S., ADHIKARI, A., SATHE, B. R., & PATEL, R. (2022). Recent Progress on Carbon Quantum Dots Based Photocatalysis. In *Frontiers in Chemistry* (Vol. 10). Frontiers Media S.A. <https://doi.org/10.3389/fchem.2022.881495>

KALANIDHI, K., & NAGARAAJ, P. (2021). Facile and Green synthesis of fluorescent N-doped carbon dots from betel leaves for sensitive detection of Picric acid and Iron ion. *Journal of Photochemistry and Photobiology A: Chemistry*, 418. <https://doi.org/10.1016/j.jphotochem.2021.113369>

LINZ, M. S., MATTAPPALLIL, A., FINKEL, D., & PARKER, D. (2023). Clinical Impact of Staphylococcus aureus Skin and Soft Tissue Infections. In *Antibiotics* (Vol. 12, Issue 3). MDPI. <https://doi.org/10.3390/antibiotics12030557>

MENG, W., BAI, X., WANG, B., LIU, Z., LU, S., & YANG, B. (2019). Biomass-Derived Carbon Dots and Their Applications. In *Energy and Environmental Materials* (Vol. 2, Issue 3, pp. 172–192). John Wiley and Sons Inc. <https://doi.org/10.1002/eem2.12038>

MOREIRA, D. R., CHAVES, P. O. B., FERREIRA, E. N., ARRUDA, T. B. M. G., RODRIGUES, F. E. A., NETO, J. F. C., PETZHOLD, C. L., MAIER, M. E., & RICARDO, N. M. P. S. (2020). Moringa polyesters as eco-friendly lubricants and its blends with naphthalenic lubricant. *Industrial Crops and Products*, 158. <https://doi.org/10.1016/j.indcrop.2020.112937>

NIE, X., JIANG, C., WU, S., CHEN, W., LV, P., WANG, Q., LIU, J., NARH, C., CAO, X., GHILADI, R. A., & WEI, Q. (2020). Carbon quantum dots: A bright future as photosensitizers for in vitro antibacterial photodynamic inactivation. *Journal of Photochemistry and Photobiology B: Biology*, 206. <https://doi.org/10.1016/j.jphotobiol.2020.111864>

ROCA, I., AKOVA, M., BAQUERO, F., CARLET, J., CAVALERI, M., COENEN, S., COHEN, J., FINDLAY, D., GYSSENS, I., HEURE, O. E., KAHLMETER, G., KRUSE, H., LAXMINARAYAN, R., LIÉBANA, E., LÓPEZ-CERERO, L., MACGOWAN, A., MARTINS, M., RODRÍGUEZ-BAÑO, J., ROLAIN, J. M., VILA, J. (2015). The global threat of antimicrobial resistance: science for intervention. *New Microbes and New Infections*, 6, 22–29. <https://doi.org/10.1016/J.NMNI.2015.02.007>

RUIZ, V., MAUDES, J., GRANDE, H. J., & PÉREZ-MARQUEZ, A. (2022). Light-activated antibacterial electrospun polyacrylonitrile-graphene quantum dot nanofibrous membranes. *Materials Today Communications*, 32. <https://doi.org/10.1016/j.mtcomm.2022.104112>

SHEN, C. L., LIU, H. R., LOU, Q., WANG, F., LIU, K. K., DONG, L., & SHAN, C. X. (2022). Recent progress of carbon dots in targeted bioimaging and cancer therapy. In *Theranostics* (Vol. 12, Issue 6, pp. 2860–2893). Ivyspring International Publisher. <https://doi.org/10.7150/thno.70721>

ST. DENIS, T. G., DAI, T., IZIKSON, L., ASTRAKAS, C., ANDERSON, R. R., HAMBLIN, M. R., & TEGOS, G. P. (2011). All you need is light, antimicrobial photoinactivation as an evolving and emerging discovery strategy against infectious disease. In *Virulence* (Vol. 2, Issue 6, pp. 509–520). Taylor and Francis Inc. <https://doi.org/10.4161/viru.2.6.17889>

UEDA YAMAGUCHI, N., CUSIOLI, L. F., QUESADA, H. B., CAMARGO FERREIRA, M. E., FAGUNDES-KLEN, M. R., SALCEDO VIEIRA, A. M., GOMES, R. G., VIEIRA, M. F., & BERGAMASCO, R. (2021). A review of Moringa oleifera seeds

in water treatment: Trends and future challenges. In *Process Safety and Environmental Protection* (Vol. 147, pp. 405–420). Institution of Chemical Engineers. <https://doi.org/10.1016/j.psep.2020.09.044>

VENTURA, A. C. S. S. B., DE PAULA, T., GONÇALVES, J. P., SOLEY, B. DA S., CRETELLA, A. B. M., OTUKI, M. F., & CABRINI, D. A. (2021). The oil from *Moringa oleifera* seeds accelerates chronic skin wound healing. *Phytomedicine Plus*, *1*(3). <https://doi.org/10.1016/j.phyplu.2021.100099>

WAINWRIGHT, M., MAISCH, T., NONELL, S., PLAETZER, K., ALMEIDA, A., TEGOS, G. P., & HAMBLIN, M. R. (2017). Photoantimicrobials—are we afraid of the light? In *The Lancet Infectious Diseases* (Vol. 17, Issue 2, pp. e49–e55). **Lancet Publishing Group**. [https://doi.org/10.1016/S1473-3099\(16\)30268-7](https://doi.org/10.1016/S1473-3099(16)30268-7)

WANG, S., LENZINI, F., CHEN, D., TANNER, P., HAN, J., THIEL, D., LOBINO, M., & LI, Q. (2023). Chemically derived graphene quantum dots for high-strain sensing. *Journal of Materials Science and Technology*, *141*, 110–115. <https://doi.org/10.1016/j.jmst.2022.08.041>

WERTHEIM, H. F. L., MELLES, D. C., VOS, M. C., VAN LEEUWEN, W., VAN BELKUM, A., VERBRUGH, H. A., & NOUWEN, J. L. (2005). The role of nasal carriage in *Staphylococcus aureus* infections. *The Lancet Infectious Diseases*, *5*(12), 751–762. [https://doi.org/10.1016/S1473-3099\(05\)70295-4](https://doi.org/10.1016/S1473-3099(05)70295-4)

WU, X., ABBAS, K., YANG, Y., LI, Z., TEDESCO, A. C., & BI, H. (2022). Photodynamic Anti-Bacteria by Carbon Dots and Their Nano-Composites. In *Pharmaceuticals* (Vol. 15, Issue 4). MDPI. <https://doi.org/10.3390/ph15040487>

WU, Y., LI, C., VAN DER MEI, H. C., BUSSCHER, H. J., & REN, Y. (2021). Carbon quantum dots derived from different carbon sources for antibacterial applications. In *Antibiotics* (Vol. 10, Issue 6). MDPI AG. <https://doi.org/10.3390/antibiotics10060623>

XIE, Y., CHENG, D., LIU, X., & HAN, A. (2019). Green hydrothermal synthesis of N-doped carbon dots from biomass highland barley for the detection of Hg²⁺. *Sensors (Switzerland)*, *19*(14). <https://doi.org/10.3390/s19143169>

YU, K., & SCHANZE, K. S. (2023). Commemorating The Nobel Prize in Chemistry 2023 for the Discovery and Synthesis of Quantum Dots. *ACS Central Science*. <https://doi.org/10.1021/acscentsci.3c01296>

ZHENG, X. T., ANANTHANARAYANAN, A., LUO, K. Q., & CHEN, P. (2015). Glowing graphene quantum dots and carbon dots: Properties, syntheses, and biological applications. In *Small* (Vol. 11, Issue 14, pp. 1620–1636). Wiley-VCH Verlag. <https://doi.org/10.1002/sml.201402648>

ZHONG, J., WANG, Y., YANG, R., LIU, X., YANG, Q., & QIN, X. (2018). The application of ultrasound and microwave to increase oil extraction from *Moringa oleifera* seeds. *Industrial Crops and Products*, *120*, 1–10. <https://doi.org/10.1016/j.indcrop.2018.04.028>

ZHUANG, P., LI, K., LI, D., QIAO, H., E, Y., WANG, M., SUN, J., MEI, X., & LI, D. (2021). Assembly of Carbon Dots into Frameworks with Enhanced Stability and

Antibacterial Activity. *Nanoscale Research Letters*, 16(1).
<https://doi.org/10.1186/s11671-021-03582-3>